



# Post-Assembly Stabilization of Rationally Designed DNA Crystals\*\*

Jiemin Zhao, Arun Richard Chandrasekaran, Qian Li, Xiang Li, Ruojie Sha, Nadrian C. Seeman,\* and Chengde Mao\*

**Abstract:** This manuscript reports an effort to stabilize self-assembled DNA crystals. Owing to their weak inter-unit cohesion, self-assembled DNA crystals are fragile, which limits the potential applications of such crystals. To overcome this problem, another molecule was introduced, which binds to the cohesive sites and stabilizes the inter-unit interactions. The extra interactions greatly improve the stability of the DNA crystals. The original DNA crystals are only stable in solutions of high ionic strength (e.g.,  $\geq 1.2\text{ M }(\text{NH}_4)_2\text{SO}_4$ ); in contrast, the stabilized crystals can be stable at ionic strengths as low as that of a  $0.02\text{ M}$  solution of  $(\text{NH}_4)_2\text{SO}_4$ . The current strategy is expected to represent a general approach for increasing the stability of self-assembled DNA nanostructures for potential applications, for example, as structural scaffolds and molecular sieves.

Self-assembly is a powerful process for the generation of a diverse range of structures and functions<sup>[1,2]</sup> that generally relies on weak, reversible interactions. If a building block attaches to an incorrect site, it can detach again because of the reversibility of the process. For such a self-correcting mechanism to work effectively, the inter-unit interactions must be sufficiently weak under the assembly conditions. However, the final structures should be stable, which requires the inter-unit interactions to be strong. Therefore, there are two conflicting requirements for the inter-unit interactions. This conflict exists in programmed DNA self-assembly as well.<sup>[3,4]</sup> Triangular DNA motifs have been engineered to assemble into macroscopic, three-dimensional (3D) crystals.<sup>[5–8]</sup> Any two adjacent triangle motifs weakly bind to each other through a pair of two-nucleotide sticky ends (single-stranded overhangs). The crystals are stable only in solutions of high ionic strength (e.g.,  $\geq 1.2\text{ M }(\text{NH}_4)_2\text{SO}_4$ ). High ionic strengths

greatly limit the applications of such self-assembled DNA frameworks. For example, gold nanoparticles will irreversibly aggregate and many enzymes will exhibit low catalytic activities under such conditions.<sup>[9,10]</sup> Overcoming this dilemma is a challenge for structural DNA nanotechnology. Herein, we have developed a strategy to address this issue by strengthening the inter-unit interactions after self-assembly.

In this work, we used weak inter-unit interactions for the self-assembly of 3D DNA crystals<sup>[5]</sup> and then added a triplex-forming oligonucleotide<sup>[11,12]</sup> to enhance the inter-unit interactions (Figure 1). With this strategy, DNA nanostructures can be assembled effectively and are stable at the same time. The key to success of this method is the formation of a DNA triplex at the inter-unit cohesion region. The DNA motif was

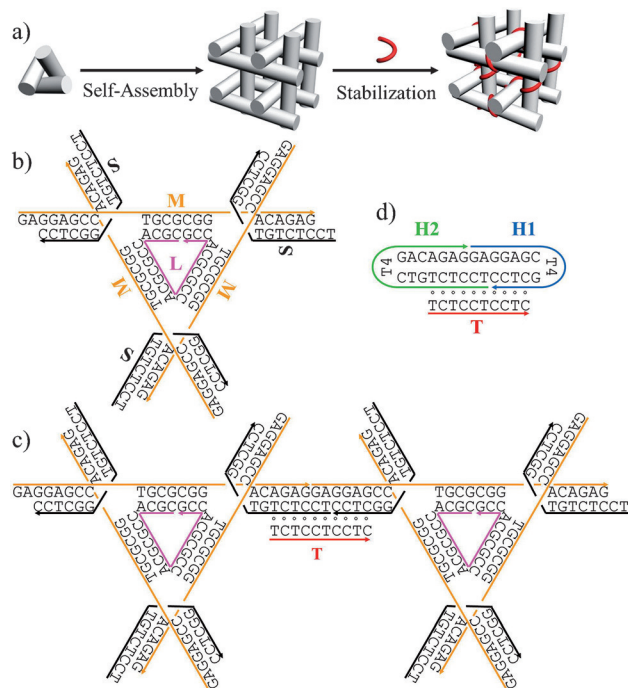


**Figure 1.** Post-assembly stabilization of DNA crystals by triplex formation. a) Overall self-assembly and stabilization process for a DNA triangle crystal. Each gray rod represents a DNA duplex, and the red line represents a triplex-forming DNA strand (T). b) DNA sequences of the tensegrity triangle. The triangle is of pseudo-threefold rotational symmetry and contains only three different types of strands: a central triply-repeating strand (L), a medium strand (M), and a short strand (S). c) Detailed interaction between two triangle motifs in the final, stabilized DNA crystal. Two triangles associate with each other by hybridization between their single-stranded overhangs (sticky ends). Such cohesion is further stabilized by triplex formation. d) A model system for testing the stabilization of the sticky-end cohesion. Two short hairpins (H1 and H2) mimic the two interacting helical domains between two triangle motifs in terms of sequences and sticky ends. Note that the cytosine (C)-containing triplex in this study forms only in acidic solution (e.g., pH 5.0).

[\*] J. Zhao, Q. Li, X. Li, Prof. C. Mao  
Department of Chemistry, Purdue University  
West Lafayette, IN 47907 (USA)  
E-mail: mao@purdue.edu

A. R. Chandrasekaran, R. Sha, Prof. N. C. Seeman  
Department of Chemistry, New York University  
New York, NY 10003 (USA)  
E-mail: ned.seeman@nyu.edu

[\*\*] This work was supported by the National Science Foundation (C.M.) and supported in part by the following grants to N.C.S.: CMMI-1120890, EFRI-1332411, and CCF-1117210 from the National Science Foundation, MURI W911NF-11-1-0024 from the Army Research Office, N000141110729 and N000140911118 from the Office of Naval Research, DE-SC0007991 from the Department of Energy for DNA synthesis and partial salary support, and grant 3849 from the Gordon and Betty Moore Foundation.

Supporting information for this article is available on the WWW under <http://dx.doi.org/10.1002/anie.201503610>.

modified from a previously reported symmetric tensegrity triangle motif.<sup>[5]</sup> It has three-fold rotational symmetry in the crystal and consists of seven DNA strands [one central triply-repeating strand (**L**), three copies of identical medium strands (**M**), and three copies of identical short strands (**S**)], which are organized into three interconnected duplexes. Each duplex contains a pair of complementary two-nucleotide sticky ends. Sticky-end hybridization allows the DNA triangle motifs to associate with each other and assemble into 3D crystals. However, the two-nucleotide sticky-end cohesion is weak and only effective in solutions of high ionic strength, for example,  $> 1.2 \text{ M}$   $(\text{NH}_4)_2\text{SO}_4$ . Herein, the sequence of the DNA duplex that connects two adjacent triangle motifs was modified in such a way that one strand is composed of only purines (A or G) while the other one is composed of only pyrimidines (T or C). At acidic pH (e.g., 5.0), this DNA duplex region can bind to a pyrimidine-only strand (**T**) to form a triplex.<sup>[13–17]</sup> Triplex formation will stabilize the sticky-end cohesion and thus the 3D crystals. The resulting DNA crystals are stable in solutions of low ionic strength, such as approximately  $0.02 \text{ M}$   $(\text{NH}_4)_2\text{SO}_4$ .

We have tested the stabilizing effect with a simple model system (Figure 1d) by native polyacrylamide gel electrophoresis (PAGE). In this system, a pair of short hairpins (**H1** and **H2**) were designed to have exactly the same sequences as the two interacting helical domains between two tensegrity triangles and thus mimic the sticky-end cohesion in the crystal assembly. An individual, cohesive two-nucleotide sticky-end is not stable at low ionic strength (e.g.,  $10 \text{ mM}$   $\text{Mg}^{2+}$ ). The two hairpins do not associate with each other and appear as two separate bands in PAGE analysis (Figure 2a). However, under acidic conditions (pH 5.0), a pyrimidine-only oligonucleotide (strand **T**) can bind to the nick-containing duplex to form a triplex. The sticky-end cohesion is thus stabilized at the same ionic strength ( $10 \text{ mM}$   $\text{Mg}^{2+}$ ). Experimentally, the two hairpins (**H1** and **H2**) and the **T** strand form a three-stranded complex, which appears as a band with much higher

molecular weight than the individual strands in PAGE analysis (Figure 2b). This experiment validates our hypothesis: Triplex formation can indeed stabilize sticky-end cohesion.

DNA crystals were assembled according to a previously reported method.<sup>[5]</sup> Briefly, the three component DNA strands (**L**, **M**, and **S**) were mixed together at a molar ratio of 1:3:3 in a neutral,  $\text{Mg}^{2+}$ -containing aqueous buffer, and the resulting solution was slowly cooled down from  $95^\circ\text{C}$  to  $4^\circ\text{C}$  over two hours. The assembled DNA triangle solution was then mixed with the crystallization buffer [ $\text{MgCl}_2$  ( $10 \text{ mM}$ ), Tris-HCl ( $50 \text{ mM}$ , pH 7.5),  $(\text{NH}_4)_2\text{SO}_4$  ( $1.6 \text{ M}$ )] and incubated against an aqueous  $(\text{NH}_4)_2\text{SO}_4$  solution ( $1.6 \text{ M}$ ) in a hanging-drop setup at  $22^\circ\text{C}$ . As the water evaporated from the DNA solution drop, both DNA and salt concentration increased, and DNA triangle crystals appeared after 17 hours. After 48 hours, the DNA crystals reached their maximum sizes. They were transferred into a new drop of the crystallization buffer with its pH adjusted to 5.6 and incubated for 24 hours. Then, the triplex-forming **T** strand was introduced into the crystal-containing drops, and the drops were further incubated for 48 hours to allow the **T** strand to diffuse into and bind to the crystals to form triplexes. To demonstrate the increased crystal stability, the crystal drop was incubated against a large volume of reservoir solution with an indicated ionic strength (by adjusting the  $(\text{NH}_4)_2\text{SO}_4$  concentration). During this process, the crystal-containing drops absorb water vapor. The drop volumes increase while the ionic strength decreases to eventually be the same as that of the reservoir buffer. Finally, the crystal morphology was examined by optical microscopy. Without triplex formation, the crystals started to degrade in  $(\text{NH}_4)_2\text{SO}_4$  solution from a concentration of  $1.5 \text{ M}$  and completely dissolved when the  $(\text{NH}_4)_2\text{SO}_4$  concentration decreased to  $1.2 \text{ M}$  (Figure 3). In sharp contrast, after triplex stabilization, the DNA crystals were stable at this ionic strength. In fact, the triplex-stabilized DNA crystals showed no obvious morphological changes at  $(\text{NH}_4)_2\text{SO}_4$  concentrations as low as  $0.02 \text{ M}$ . The crystals completely dissolved when incubated against water (without any salt).

We also monitored the morphological changes of the DNA crystals as a function of the incubation time (for details, see the Supporting Information, Figures S1 and S2). The time-course experiments further demonstrated the improved

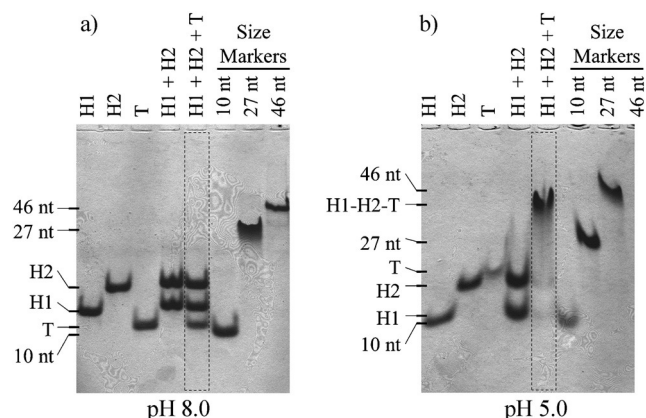


**Figure 2.** Triplex stabilization of sticky-end cohesion in a hairpin model system studied by native PAGE analysis at different pH values. The sample compositions and band identities are indicated above and beside the gel images, respectively. The lanes corresponding to potential triplex formation are highlighted by dashed boxes. Note that the mobility of the third strand itself changed significantly between the two gels, presumably because of the different protonation states of cytosine residues in solutions with different pH values.

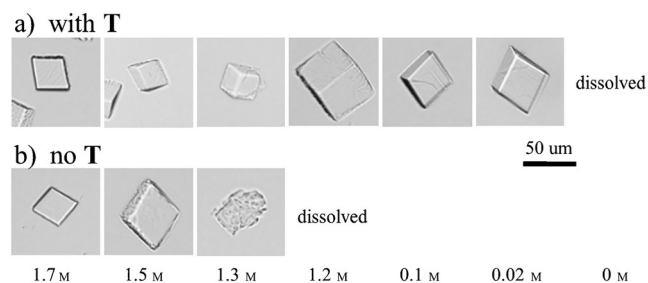


**Figure 3.** Triplex-stabilizing effect on DNA crystals investigated by optical microscopy. DNA crystals with (top) and without (bottom) the triplex-forming strand (**T**) equilibrated against buffers with different ionic strengths for 49 hours.  $(\text{NH}_4)_2\text{SO}_4$  concentrations are indicated at the bottom. In each case, the crystals are from the same drop, but not necessarily the same crystals.

crystal stability after triplex formation. For example, the DNA crystals after triplex formation showed no observable changes when kept in a 1.0 M  $(\text{NH}_4)_2\text{SO}_4$  solution for 74 hours, whereas the DNA crystals without triplex stabilization dissolved within 34 hours. An even more dramatic difference was seen at lower  $(\text{NH}_4)_2\text{SO}_4$  concentrations. For example, in 0.02 M  $(\text{NH}_4)_2\text{SO}_4$  solution, DNA crystals with triplex stabilization showed no signs of degradation over 74 hours, whereas the DNA crystals without triplex formation completely dissolved in 6 hours. Furthermore, two control experiments were performed. Strand **T** at pH 8.0 (Figure S3) or a non-triplex-forming strand **T'** at pH 5.6 (Figure S4) were added to DNA crystals before incubating the crystals against different concentrations of  $(\text{NH}_4)_2\text{SO}_4$ . Under both conditions, triplexes cannot be formed, and therefore, no stabilization is expected; this hypothesis was clearly supported by the experimental data.

To confirm that the triplex indeed formed in the DNA crystals, we used denaturing PAGE analysis to determine the composition of the DNA crystals (Figure 4). After incubation with or without the **T** strand at pH 5.6 or 8.0 for 48 hours, the DNA crystals were extensively washed to remove any free **T** strands. The DNA crystals were then dissolved, and their component DNA strands were analyzed by denaturing PAGE. In the gel image, the **T** strand was absent in the crystal sample incubated at pH 8.0 because it could not bind to the triangles by triplex formation. However, for the DNA crystals kept at pH 5.6, a band corresponding to the **T** strand was clearly visible. This observation indicated that at acidic pH, the **T** strand indeed bound to the DNA crystals through pH-dependent triplex formation. To gain more quantitative

insights, we determined the ratio of the DNA strands by measuring the intensity of each band to estimate how many potential triplex-forming sites actually formed triplexes. We found that in the crystals, approximately 50 % of the sticky-end cohesions were stabilized by triplex formation. Even though this quantification method provides only a rough estimate, it strongly suggested that even partial triplex formation (or stabilization of some of the inter-motif interactions) significantly stabilized the DNA crystals.

To further confirm the triplex formation, we labeled the **T** strand with a red dye, **Cy3**, at its 5' end. If the new **T-Cy3** strands bind to the DNA crystals, they will change their color to red. Optical images clearly confirmed this hypothesis (Figure 5) and corroborated that the stabilization of the DNA crystals was due to triplex formation.

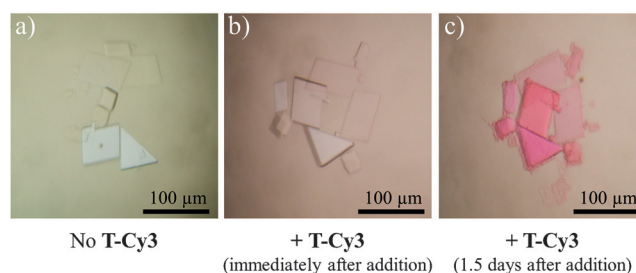


**Figure 5.** Optical visualization of the binding of the **T** strand to the DNA crystals. The modified strand **T-Cy3** has exactly the same sequence but with a red dye, **Cy3**, at the 5' end. Incorporation of the **T-Cy3** strand introduces red color into the previously colorless DNA crystals.

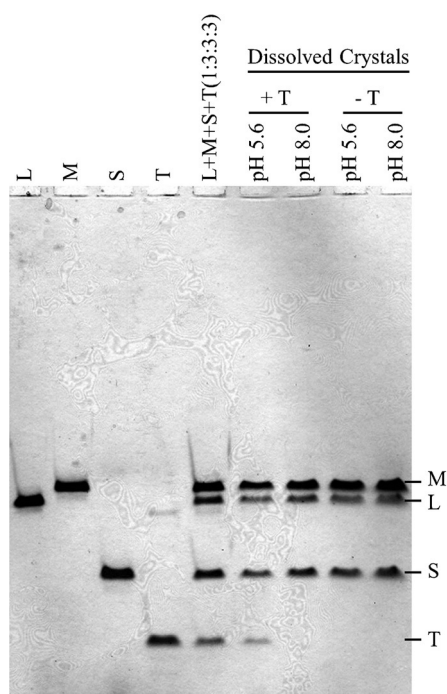


**Figure 4.** Denaturing PAGE analysis of the composition of the stabilized DNA crystals. The chemical composition of each lane and the chemical identity of each band are indicated above and beside the gel image, respectively.

In conclusion, we have developed a strategy for the stabilization of self-assembled DNA crystals by strengthening the inter-unit interactions after crystal assembly. Although the current stabilization method relies on triplex formation at acidic pH, it should be straightforward to form triplexes at neutral pH by introducing triplex-stabilizing modified bases, for example, by replacing C and T with 2'-aminoethoxy-methyl-C and 2'-aminoethoxy-T, respectively.<sup>[18]</sup> Along with the concept of post-assembly stabilization, it is also conceivable to introduce other sequence-specific stabilization motifs at the sites of sticky-end cohesion, for example, by sequence-specific protein binding or polyamide recognition.<sup>[19,20]</sup> The significance of this work lies in the fact that a solution environment similar to physiological conditions can now be used for DNA crystals. In such an environment, potential guests behave more as they would in their native conditions. For example, enzymes will have higher activities,<sup>[10]</sup> and inorganic nanoparticles will be less likely to aggregate irreversibly.<sup>[9]</sup> Further studies along this line are currently being conducted by our groups.

**Keywords:** crystal engineering · DNA structures · nanostructures · self-assembly

**How to cite:** *Angew. Chem. Int. Ed.* **2015**, 54, 9936–9939  
*Angew. Chem.* **2015**, 127, 10074–10077

- 
- [1] G. M. Whitesides, J. P. Mathias, C. T. Seto, *Science* **1991**, *254*, 1312–1319.
- [2] J. M. Lehn, *Proc. Natl. Acad. Sci. USA* **2003**, *99*, 4763–4768.
- [3] N. C. Seeman, *Annu. Rev. Biochem.* **2010**, *79*, 65–87.
- [4] E. Winfree, F. R. Liu, L. A. Wenzler, N. C. Seeman, *Nature* **1998**, *394*, 539–544.
- [5] J. P. Zheng, J. J. Birktoft, Y. Chen, T. Wang, R. J. Sha, P. E. Constantinou, S. L. Ginell, C. D. Mao, N. C. Seeman, *Nature* **2009**, *461*, 74–77.
- [6] T. Wang, R. J. Sha, J. Birktoft, J. P. Zheng, C. D. Mao, N. C. Seeman, *J. Am. Chem. Soc.* **2010**, *132*, 15471–15473.
- [7] D. G. Liu, M. S. Wang, Z. X. Deng, R. Walulu, C. D. Mao, *J. Am. Chem. Soc.* **2004**, *126*, 2324–2325.
- [8] D. A. Rusling, A. R. Chandrasekaran, Y. P. Ohayon, T. Brown, K. R. Fox, R. J. Sha, C. D. Mao, N. C. Seeman, *Angew. Chem. Int. Ed.* **2014**, *53*, 3979–3982; *Angew. Chem.* **2014**, *126*, 4060–4063.
- [9] X. G. Han, J. Goebel, Z. D. Lu, Y. D. Yin, *Langmuir* **2011**, *27*, 5282–5289.
- [10] J. C. Warrant, S. G. Cheatum, *Biochemistry* **1966**, *5*, 1702–1707.
- [11] A. Jain, G. L. Wang, K. M. Vasquez, *Biochimie* **2008**, *90*, 1117–1130.
- [12] K. M. Vasquez, P. M. Glazer, *Q. Rev. Biophys.* **2002**, *35*, 89–107.
- [13] N. Sugimoto, P. Wu, H. Hara, Y. Kawamoto, *Biochemistry* **2001**, *40*, 9396–9405.
- [14] Z. Y. Liu, Y. M. Li, C. Tian, C. D. Mao, *Biomacromolecules* **2013**, *14*, 1711–1714.
- [15] Y. Chen, S. H. Lee, C. D. Mao, *Angew. Chem. Int. Ed.* **2004**, *43*, 5335–5338; *Angew. Chem.* **2004**, *116*, 5449–5452.
- [16] A. Idili, A. Vallée-Bélisle, F. Ricci, *J. Am. Chem. Soc.* **2014**, *136*, 5836–5839.
- [17] A. Amodio, B. Zhao, A. Porchetta, A. Idili, M. Castronovo, C. H. Fan, F. Ricci, *J. Am. Chem. Soc.* **2014**, *136*, 16469–16472.
- [18] S. Buchini, C. J. Leumann, *Tetrahedron Lett.* **2003**, *44*, 5065–5068.
- [19] J. S. Kang, J. L. Meier, P. B. Dervan, *J. Am. Chem. Soc.* **2014**, *136*, 3687–3694.
- [20] J. M. Gottesfeld, C. Melander, R. K. Suto, H. Raviol, K. Luger, P. B. Dervan, *J. Mol. Biol.* **2001**, *309*, 615–629.
- Received: April 20, 2015  
Revised: June 5, 2015  
Published online: July 1, 2015
-